resulting from the decomposition of $Os_4(CO)_{14}(PF_3)_2$. It would be expected that $Os_4(CO)_{14}(PF_3)_2$ would be less stable than **2**, given that **2** is less stable than **1**.

As we have mentioned above, **1** is apparently an intermediate in the decomposition of $Os_2(CO)_9$ to $Os_3(CO)_{12}$. Further support for the mechanism in eq 3 is that ethylene readily undergoes reversible dissociation from $Os_2(CO)_8(\mu\text{-}C_2H_4)$.[40]

(40) (a) Hembre, R. T.; Scott, C. P.; Norton, J. R. *J. Am. Chem. Soc.* **1987**, *109*, 3468. (b) Takats, J. *Polyhedron* **1988**, *7*, 931.

Acknowledgment. We thank the Natural Sciences and Engineering Research Council of Canada for financial support.

Note Added in Proof. Extended Hückel molecular orbital calculations on **1** have been reported: Mealli, C.; Proserpio, D. M. *J. Am. Chem. Soc.* **1990**, *112*, 5484.

Supplementary Material Available: Tables of hydrogen atom coordinates for **3** and anisotropic thermal parameters for **1**, **2**, and **3** (4 pages); listings of observed and calculated structure factors for **1**, **2**, and **3** (65 pages). Ordering information is given on any current masthead page.

Decomposition of (α-Phenethyl)bis(dimethylglyoximato)cobalt(III) Complexes. Influence of Electronic and Steric Factors on the Kinetics and Thermodynamics of Cobalt–Carbon Bond Dissociation

Flora T. T. Ng,*[1a,b] Garry L. Rempel,[1a,b] Curt Mancuso,[1b] and Jack Halpern*[1b]

Department of Chemistry, The University of Chicago, Chicago, Illinois 60637, and Department of Chemical Engineering, University of Waterloo, Waterloo, Ontario, Canada N2L 3G1

Received March 14, 1990

(α-Phenethyl)bis(dimethylglyoximato)cobalt(III) complexes were found to undergo reversible decomposition reactions according to

$$C_6H_5CH(CH_3)\text{—}Co(DH)_2B \rightleftharpoons Co^{II}(DH)_2B + C_6H_5CH{=}CH_2 + \tfrac{1}{2}H_2$$

which attained measurable equilibria under ca. 1 atm of H_2. The kinetics and, in some cases, equilibria of these reactions were determined for a series of complexes containing different trans-axial ligands B (pyridine (py), 4-CH_3-py, 4-NH_2-py, 4-CN-py, 2-CH_3-py, 2-NH_2-py, imidazole, 2-NH_2CH_2-py, 2-$NH_2CH_2CH_2$-py, aniline, acetone). In the presence of the free-radical trap 2,2,6,6-tetramethylpiperidinyl-1-oxy (Tempo), an additional pathway of decomposition of $C_6H_5CH(CH_3)$–$Co(DH)_2$py was observed that yielded the $C_6H_5\dot{C}H(CH_3)$ radical–Tempo adduct according to

$$C_6H_5CH(CH_3)\text{–}Co(DH)_2py + Tempo \rightarrow Co^{II}(DH)_2py + C_6H_5CH(CH_3)\text{–}Tempo$$

Homolytic Co–C bond dissociation energies, $D_{Co\text{–}C}$, were deduced from measurements of ΔH and $\Delta H^{\ddagger}$ of these reactions and ranged from 17 kcal/mol for B = 2-NH_2-py to 21 kcal/mol for B = 4-NH_2-py. The variations in $D_{Co\text{–}C}$ and in the rates of Co–C bond homolysis were interpreted in terms of the electronic and steric influences of B. Thus, for constant steric influences, $D_{Co\text{–}C}$ increases with the electron-donor ability (pK_a) of B, whereas for constant pK_a, $D_{Co\text{–}C}$ decreases with increasing steric bulk of B. The above reactions proceed through a common rate-determining step, namely, homolysis of the Co–C bond.

Introduction

This paper describes a study of the kinetics and thermodynamics of the Co–C bond dissociation reactions of a series of (α-phenethyl)bis(dimethylglyoximato)cobalt(III) complexes containing different trans-axial ligands. The influences of electronic and steric properties of the latter are examined, along with the influence on the kinetics and product distribution of the free-radical trap 2,2,6,6-tetramethylpiperidinyl-1-oxy (Tempo).

Our studies encompass the determination of the kinetics and equilibrium constants of the reactions depicted by eq 1 (where DH_2 = dimethylglyoxime and B = axial base ligand such as pyridine (py), substituted pyridine, imidazole, aniline, etc.) We have found that certain such reactions (e.g., where B = py, substituted pyridine) attain a readily measurable equilibrium at ambient temperatures under H_2 pressures of ca. 1 atm. The reactions corresponding to the reverse of eq 1 and analogues thereof (including variants involving the addition of "cobalt hydrides" to activated olefins) have previously been recognized as synthetic routes to organocobalt compounds, including organocobalamins.[2-6] The decomposition of other alkylcobalt compounds to yield olefins also is well documented qualitatively.[3,7,8]

$$\underset{\mathbf{1}}{C_6H_5CH(CH_3)\text{—}Co(DH)_2B} = \underset{\mathbf{2}}{Co^{II}(DH)_2B} + C_6H_5CH{=}CH_2 + \tfrac{1}{2}H_2 \quad (1)$$

(1) (a) University of Waterloo. (b) The University of Chicago.

(2) Johnson, A. W.; Mervyn, L.; Shaw, N.; Lester Smith, E. *J. Chem. Soc.* **1963**, 4146.
(3) Schrauzer, G. N.; Windgassen, R. J. *J. Am. Chem. Soc.* **1967**, *89*, 1999.
(4) Schrauzer, G. N.; Holland, R. J. *J. Am. Chem. Soc.* **1971**, *93*, 1505, 4060.
(5) Simandi, L. I.; Szeverenyi, Z.; Budo-Zahoni, E. *Inorg. Nucl. Chem. Lett.* **1975**, *11*, 773.
(6) Simandi, L. I.; Budo-Zahoni, E.; Szeverenyi, Z.; Nemeth, S. *J. Chem. Soc., Dalton Trans.* **1980**, 276.
(7) Schrauzer, G. N.; Sibert, J. W.; Windgassen, R. J. *J. Am. Chem. Soc.* **1968**, *90*, 6681.

0276-7333/90/2309-2762$02.50/0

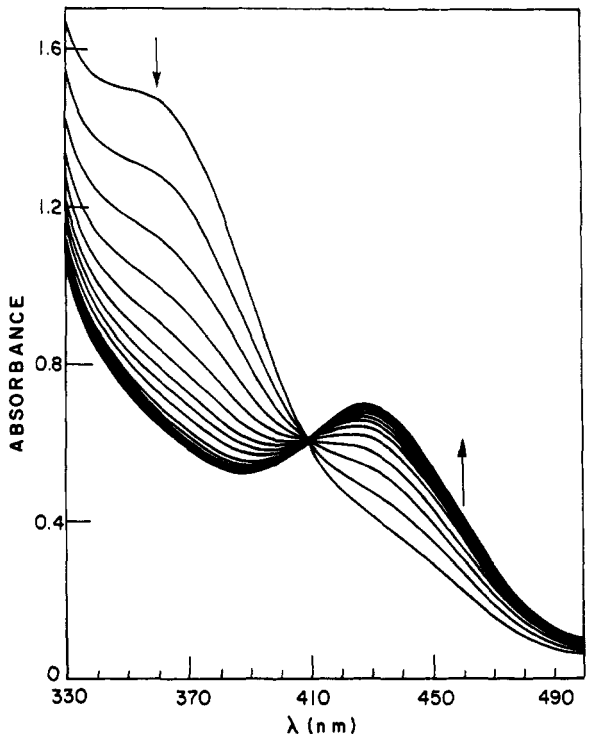

Figure 1. Representative spectral changes accompanying the decomposition of $C_6H_5CH(CH_3)$–$Co(DH)_2(4\text{-}CH_3\text{-py})$ (initially ca. 2×10^{-4} M) in acetone under Ar at 34.5 °C. The spectra were recorded at 2-min intervals (cell path length 1 cm).

In the presence of the free-radical trap Tempo (3), an additional decomposition pathway was observed, leading to the formation of $C_6H_5CH(CH_3)$–Tempo (4) in accord with eq 2. Measurements of the kinetics of the latter

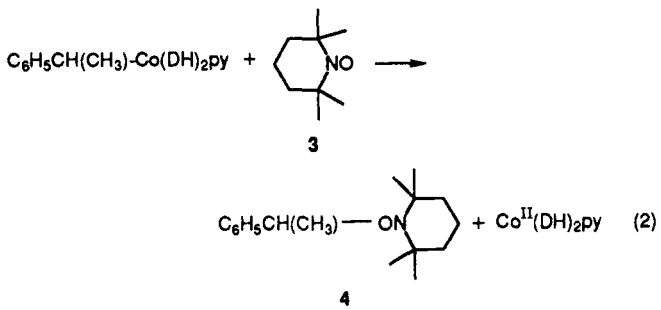

(2)

reaction yield values for the Co–C bond dissociation energy of 1 and provide insight into the mechanism of reaction 1.

The results of this study are of relevance to various themes in organometallic chemistry and catalysis, as well as to certain biological systems, notably biochemical rearrangements promoted by coenzyme B_{12} (5′-deoxyadenosylcobalamin).[9,10] It now is widely accepted that these reactions proceed through free-radical mechanisms triggered by enzyme-induced homolytic dissociation of the cobalt–carbon bond of the coenzyme to generate a 5′-deoxyadenosyl radical.[10-13] Accordingly, there is considerable interest in understanding the factors that influence cobalt–carbon bond dissociation energies and that may contribute to enzyme-induced cobalt–carbon bond weakening and dissociation.

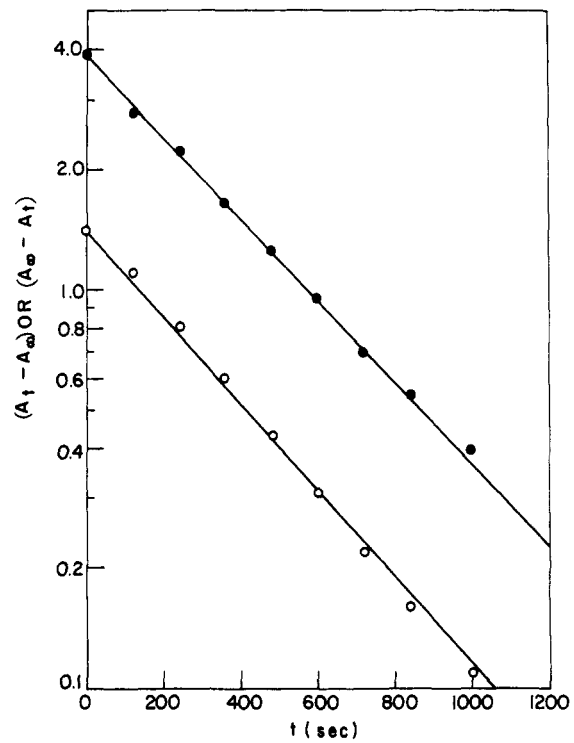

Figure 2. Representative first-order plots for the decomposition of $C_6H_5CH(CH_3)$–$Co(DH)_2(4\text{-}CH_3\text{-py})$ (initially ca. 2×10^{-4} M) in acetone under Ar at 34.5 °C: (○) 430 nm; (●) 350 nm.

In earlier preliminary communications[14-16] we have described the application of measurements of the thermodynamics and kinetics of reaction 1 to the determination of the cobalt–carbon bond dissociation energies of a series of $C_6H_5CH(CH_3)$–$Co(DH)_2B$ compounds. The present paper elaborates and extends these studies. Attention also is directed to several other recent investigations of these and closely related systems.[17-21]

Results

Decomposition in the Absence of Added Tempo. Stoichiometry and Products. In the absence of H_2 (i.e., under an atmosphere of N_2 or Ar) decomposition of $C_6H_5CH(CH_3)$–$Co(DH)_2B$ in toluene or acetone in the dark, according to eq 1, proceeds to completion. The expected stoichiometry was confirmed by characterization of the products, spectral matching, GLC, NMR spectroscopy, and gas evolution measurements.[22]

(8) Duong, K. N. V.; Ahond, A.; Merienne, C.; Gaudemer, A. *J. Organomet. Chem.* **1973**, *55*, 375.
(9) Halpern, J. *Pure Appl. Chem.* **1986**, *58*, 475.
(10) Halpern, J. In B_{12}; Dolphin, D., Ed.; Wiley: New York, 1982; Vol. 1, p 501, and references therein.
(11) Halpern, J. *Science* **1985**, *227*, 869 and references therein.
(12) Abeles, R. H.; Dolphin, D. *Acc. Chem. Res.* **1976**, *9*, 114 and references therein.
(13) Babior, B. M. *Acc. Chem. Res.* **1975**, *8*, 376 and references therein.
(14) Halpern, J.; Ng, F. T. T.; Rempel, G. L. *J. Am. Chem. Soc.* **1979**, *101*, 7124.
(15) Ng, F. T. T.; Rempel, G. L.; Halpern, J. *J. Am. Chem. Soc.* **1982**, *104*, 621.
(16) Ng, F. T. T.; Rempel, G. L.; Halpern, J. *Inorg. Chim. Acta* **1983**, *77*, L165 and references therein.
(17) Nishinaga, A.; Nishizawa, K.; Nakayama, Y.; Matsura, T. *Tetrahedron Lett.* **1977**, 85.
(18) Gjerde, H. B. G.; Espenson, J. H. *Organometallics* **1982**, *1*, 435.
(19) Derenne, S.; Gaudemer, A.; Johnson, M. D. *J. Organomet. Chem.* **1987**, *322*, 229.
(20) Derenne, S.; Gaudemer, A.; Johnson, M. D. *J. Organomet. Chem.* **1987**, *322*, 239.
(21) Baldwin, D. A.; Betterton, E. A.; Chemaly, S. M.; Pratt, J. M. *J. Chem. Soc., Dalton Trans.* **1985**, 1613.
(22) In one case, namely the thermolysis of $C_6H_5CH(CH_3)$–$Co(DH)_2(H_2O)$ in acetone, the total amount of H_2 evolved established by GLC was lower than that expected from the stoichiometry represented by eq 1. This is attributable to the more facile irreversible reduction of $Co^{II}(DH)_2(H_2O)$ in acetone compared with that of $Co(DH)_2(py)$.[5,6] Indirect support for this was provided by the observation that for $C_6H_5CH(CH_3)$–$Co(DH)_2(H_2O)$ in acetone under H_2, even at 25 °C, the equilibrium of eq 1 was unstable, presumably due to the irreversible reduction of $Co^{II}(DH)_2(H_2O)$ in acetone by H_2.[4,5]

Table I. Summary of the Kinetic and Thermodynamic Parameters for the Decomposition of $C_6H_5CH(CH_3)$–$Co(DH)_2B$ Complexes at 25 °C in Acetone under N_2 or Ar

B	pK_a[24]	10^4k_0, s^{-1}	10^6K_0, $M^{3/2}$	$\Delta H^{\ddagger}_0$, kcal mol^{-1}	$\Delta S^{\ddagger}_0$, cal mol^{-1} K^{-1}	ΔH_0, kcal mol^{-1}	ΔS_0, cal mol^{-1} K^{-1}	D_{Co-C},[e] kcal mol^{-1}	$\Delta H^{\ddagger}_0 - D_{Co-C}$, kcal mol^{-1}
4-NH_2-py	9.1	3.97[a]	5.51[a]	23.1 ± 0.3	3.8 ± 0.3	23.4 ± 0.7	54.3 ± 2.3	21.2	1.9
4-NH_2-py[b]	9.1	3.83							
imidazole	7.0	1.73	3.96[a]	23.0 ± 0.5	1.9 ± 1.8	23.0 ± 0.4	52.5 ± 2.3	20.8	2.2
2-NH_2-py[c]	6.7	81.2	193	17.7 ± 0.9	−8.2 ± 3.0	18.8 ± 0.3	46.2 ± 0.9	16.6	1.1
4-CH_3-py	6.3	6.03[a]	13.6[a]	21.8 ± 0.5	0.9 ± 1.6	22.3 ± 0.8	52.5 ± 2.6	20.1	1.7
2-CH_3-py	6.0	10.6							
py	5.2	7.34	19.5	21.6 ± 0.3	−0.2 ± 1.1	21.7 ± 0.6	54.1 ± 2.0	19.5	2.1
py[b]	5.2	7.80	13.6	21.2 ± 0.5	−1.4 ± 1.5	22.1 ± 0.5	51.9 ± 1.6	19.9	1.3
4-CN-py	1.7	13.1	47.2[a]	20.1 ± 0.6	−3.9 ± 1.8	20.1 ± 0.6	47.5 ± 2.1	17.9	2.2
4-CN-py[b]	1.7	15.0		19.4 ± 0.5	−6.1 ± 1.7				
acetone[d]	−7.2	24.6	1330	19.1 ± 0.7	−6.1 ± 2.4	19.1 ± 0.8	50.9 ± 2.8	16.9	2.2

[a] Value obtained from respective Arrhenius or van't Hoff plots. [b] Measurements in toluene; data for py from ref 14. [c] Values for the decomposition of undissociated $C_6H_5CH(CH_3)$–$Co(DH)_2$(2-NH_2-py). [d] Formed in situ by solvent displacement of H_2O from $C_6H_5CH(CH_3)$–$Co(CH)_2(H_2O)$. [e] Computed from ΔH_0 by means of eq 24 with $\Delta H_f(C_6H_5CH(CH_3)) = 33$ kcal mol^{-1} and $\Delta H_f(C_6H_5CH{=}CH_2) = 35.2$ kcal mol^{-1}.

Kinetics of Decomposition of Complexes Containing 4-Substituted Pyridines and Imidazole. The kinetics of the thermal decomposition of $C_6H_5CH(CH_3)$–$Co(DH)_2B$ (B = 4-CH_3-py, 4-NH_2-py, 4-CN-py, py, imidazole) under N_2 or Ar in acetone or toluene were determined over the temperature range 10–45 °C and found to conform to the first-order rate law shown by eq 3. A

$$-d[C_6H_5CH(CH_3)\text{–}Co(DH)_2B]/dt = d[Co^{II}(DH)_2B]/dt = k_0[C_6H_5CH(CH_3)\text{–}Co(DH)_2B] \quad (3)$$

representative time-dependent sequence of spectra for the decomposition of $C_6H_5CH(CH_3)$–$Co(DH)_2$(4-CH_3-py) in acetone is shown in Figure 1. Similar spectral changes were observed for the decomposition of other $C_6H_5CH(CH_3)$–$Co(DH)_2B$ complexes, which in each case exhibited an isosbestic point at ~400–420 nm, reflecting the decrease of absorbance of $C_6H_5CH(CH_3)$–$Co(DH)_2B$ at 350–360 nm and a parallel increase of the absorbance of $Co^{II}(DH)_2B$ at 430–460 nm. First-order plots of log $|A_t - A_\infty|$ vs time at 350–360 nm (or log $|A_\infty - A_t|$ vs time at 430–460 nm), exemplified by those in Figure 2, were linear for several half-lives. Values of k_0 (defined by eqs 1 and 3), derived from the slopes of such first-order plots, were reproducible to within 10%. The values of k_0 obtained from an analysis of absorbance changes at 350–360 nm and at 430–460 nm, respectively, were in good agreement. Values of k_0 at 25 °C for the decomposition of $C_6H_5CH(CH_3)$–$Co(DH)_2B$ complexes are listed in Table I. These values are independent of the initial concentration of $C_6H_5CH(CH_3)$–$Co(DH)_2B$ from ~10^{-3} to 2.2×10^{-4} M for B = py and 4-NH_2-py (Appendix A, supplementary material) and, in the case of $C_6H_5CH(CH_3)$–$Co(DH)_2$py, of added $Co^{II}(DH_2)$py up to 6.8×10^{-4} M.

The temperature dependencies of the rates of decomposition of several $C_6H_5CH(CH_3)$–$Co(DH)_2B$ complexes are reported in Appendix A (supplementary material). The data yielded excellent Eyring plots, from which the values of $\Delta H^{\ddagger}_0$ and $\Delta S^{\ddagger}_0$ in Table I were determined. An independent determination[23] of $\Delta H^{\ddagger}_0$ and $\Delta S^{\ddagger}_0$ for the decomposition of $C_6H_5CH(CH_3)$–$Co(DH)_2$py in acetone over the temperature range 10–30 °C yielded the values 20.9 ± 0.4 kcal mol^{-1} and −2 ± 2 cal mol^{-1} K^{-1}, respectively, in good agreement with the values 21.6 ± 0.3 kcal mol^{-1} and −0.2 ± 1.1 cal mol^{-1} K^{-1} obtained in the present study.

Table II. Effect of Added 4-Substituted Pyridines, B, on k_0 for the Decomposition of $C_6H_5CH(CH_3)$–$Co(DH)_2B$ (Initially ca. 2×10^{-4} M) in Acetone under N_2 at 25 °C

B	added [B], M	k_0, s^{-1}	λ_{max}(final spectrum), nm
4-CN-py	0	1.2×10^{-3}[a]	430
4-CN-py	0.06	1.2×10^{-3}	420
4-NH_2-Py	0	3.8×10^{-4}[a]	430
4-NH_2-py	0.11	3.8×10^{-4}	430
py	0	8.0×10^{-4}[a]	425
py	0.1	8.2×10^{-4}	425, 470 (s)[c]
py	0.05	9.1×10^{-4}[b]	425, 470 (s)

[a] These k_0 values differ slightly from those shown in Table I, since they were determined at the time of the added B experiments for purposes of uniform comparison. [b] T = 25.5 °C. [c] s = shoulder.

Scheme I

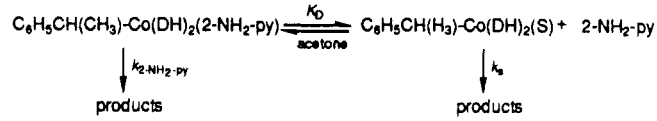

Adding excess base, B (B = 4-NH_2-py, 4-CN-py, py), to the corresponding $C_6H_5CH(CH_3)$–$Co(DH)_2B$ complexes in acetone at 25 °C under N_2 had essentially no effect on the value of k_0 (Table II), although some effect on the final spectra of the "$Co^{II}(DH)_2B$" decomposition products was noted (possibly reflecting formation of some $Co^{II}(DH)_2B_2$).

Effect of Solvent on k_0 and Activation Parameters. Nearly identical k_0 values were obtained for the decomposition of $C_6H_5CH(CH_3)$–$Co(DH)_2B$ (B = py, 4-CN-py, 4-NH_2-py) in toluene and acetone. Where determined (B = py, 4-CN-py), the activation parameters also were nearly identical (Table I).

Kinetics of Decomposition of $C_6H_5CH(CH_3)$–$Co(DH)_2$(S) in Acetone (S = H_2O, Acetone). Good first-order kinetics were observed for the thermal decomposition of $C_6H_5CH(CH_3)$–$Co(DH)_2(H_2O)$ in acetone. In view of the demonstrated lability of the H_2O ligand in $RCo(DH)_2(H_2O)$ complexes,[25,26] it seems likely that the measured k_0 values refer to $C_6H_5CH(CH_3)$–$Co(DH)_2$(acetone); i.e., S = acetone.

(23) Mancuso, C. Ph.D. Dissertation, The University of Chicago, 1990.
(24) Smith, R. M.; Martell, A. E. *Stability Constants*; Plenum Press: New York, 1975; Vol. 2. pK_a of 4-CN-py obtained from: *Stability Constants*; Special Publication 25; The Chemical Society: London, 1971; Supplement No. 1. pK_a of acetone obtained from: Gordon, J. E. *Organic Chemistry of Electrolyte Solutions*; Wiley: New York, 1975; p 156.
(25) (a) Brown, K. L.; Lylas, D.; Pencovici, M.; Kallen, R. G. *J. Am. Chem. Soc.* **1975**, *97*, 7338. (b) Brown, K. L.; Awtrey, A. W. *Inorg. Chem.* **1978**, *17*, 111.
(26) Bersciani-Pahor, N.; Forcolin, M.; Marzilli, L. G.; Randaccio, L.; Summers, M. F.; Toscano, P. J. *Coord. Chem. Rev.* **1985**, *63*, 1.

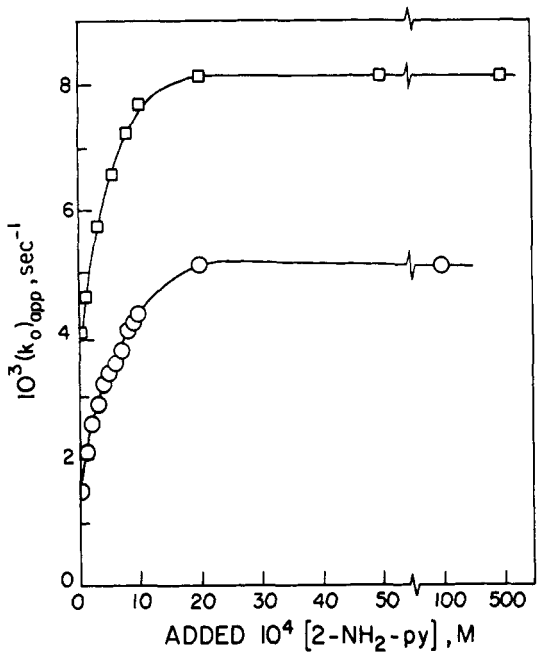

Figure 3. Effect of added 2-NH_2-py on the rate of decomposition of $C_6H_5CH(CH_3)$–$Co(DH)_2B$ (initially ca. 2×10^{-4} M) in acetone under N_2: (○) 20 °C, B = acetone; (□) 25 °C, B = 2-NH_2-py.

The final spectra, following complete decomposition of $C_6H_5CH(CH_3)$–$Co(DH)_2$(S), corresponded to that of $Co^{II}(DH)_2$ in acetone.[27]

Kinetics of Decomposition of $C_6H_5CH(CH_3)$–$Co(DH)_2B$ (B = 2-Substituted Pyridine). In an attempt to examine the steric influences of B, the decomposition of $C_6H_5CH(CH_3)$–$Co(DH)_2$(2-NH_2-py) was studied in acetone under N_2. Good first-order kinetics were observed. However, addition of excess 2-NH_2-py to $C_6H_5CH(CH_3)$–$Co(DH)_2$(2-NH_2-py) increased the value of $(k_0)_{app}$, approaching a limiting value (k_0) at $>2 \times 10^{-3}$ M 2-NH_2-py (Figure 3; Appendix B (supplementary material)). The data are consistent with Scheme I.

Assuming a rapid equilibrium between $C_6H_5CH(CH_3)$–$Co(DH)_2$(2-NH_2-py) and $C_6H_5CH(CH_3)$–$Co(DH)_2$(S), the relation between $(k_0)_{app}$ and the individual rate constants and dissociation constant, K_D, is given by eq 4,[28]

$$\frac{1}{(k_0)_{app} - k_s} = \frac{1}{k_{2\text{-}NH_2\text{-}py} - k_s} + \frac{K_D}{(k_{2\text{-}NH_2\text{-}py} - k_s)[2\text{-}NH_2\text{-}py]} \quad (4)$$

where k_s refers to the rate constant for the decomposition of $C_6H_5CH(CH_3)$–$Co(DH)_2$(S), i.e. $C_6H_5CH(CH_3)$–$Co(DH)_2(H_2O)$ in acetone (Table I and Appendix A, supplementary material). From the slope and intercept of the plot of $((k_0)_{app} - k_s)^{-1}$ vs added [2-NH_2-py]$^{-1}$ in Figure 4[29] (7.4×10^{-2} M s^{-1} and 1.5×10^{-2} s, respectively), $k_{2\text{-}NH_2\text{-}py}$ was determined to be 9.1×10^{-3} s^{-1}, in satisfactory agreement with the limiting value of 8.1×10^{-3} s^{-1} from Figure 3. The value of the dissociation equilibrium constant, K_D, for $C_6H_5CH(CH_3)$–$Co(DH)_2$(2-NH_2-py) at 25 °C was calculated to be 5.1×10^{-4} M. Corresponding measurements at 20 °C yielded $k_{2\text{-}NH_2\text{-}py} = 5.2 \times 10^{-3}$ s^{-1} and $K_D = 3.4 \times 10^{-4}$ M (Figures 3 and 4, Appendix B, supplementary material). Measurement of k_0 (limiting values at high [2-NH_2-py]) at temperatures ranging from 5 to 25 °C yielded $\Delta H^{\ddagger}_0 = 17.7 \pm 0.9$ kcal mol^{-1} and $\Delta S^{\ddagger}_0 = -8.2 \pm 3.0$ cal mol^{-1} K^{-1} (Table I, Appendix B, supplementary material).

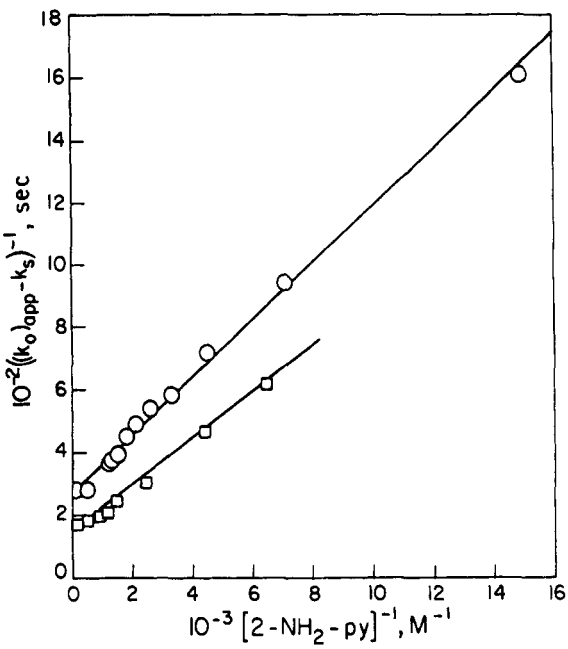

Figure 4. Effect of added 2-NH_2-py on the rate of decomposition of $C_6H_5CH(CH_3)$–$Co(DH)_2B$ (initially ca. 2×10^{-4} M) in acetone under N_2 (plot of $(k_{obs} - k_s)^{-1}$ vs [2-NH_2-py]$^{-1}$ corrected for dissociation of $C_6H_5CH(CH_3)$–$Co(DH)_2$(2-NH_2-py)): (○) 20 °C, B = acetone; (□) 25 °C, B = 2-NH_2-py).

Table III. Rate Constants for the Decomposition of $C_6H_5CH(CH_3)$–$Co(DH)_2B$ Complexes Prepared by Addition of B to $C_6H_5CH(CH_3)$–$Co(DH)_2(H_2O)$ (Initially ca. 2×10^{-4} M) in Acetone under N_2 at 25 °C

added B	added [B], M	pK_a	$10^4(k_0)_{app}$,[a] s^{-1}
none			24.6
2-NH_2-py	≥0.002	6.7[24,30]	81.2*
2-CH_3-py	0.001	5.95[24]	22.0
2-CH_3-py	0.005	5.95[24]	19.1
2-CH_3-py	0.01	5.95[24]	13.3
2-CH_3-py	0.05	5.95[24]	10.9*
2-CH_3-py	0.10	5.95[24]	10.1*
2-CH_3-py	0.30	5.95[24]	10.7*
2-CH_3-py	1.0	5.95[24]	10.7*
2-AMP	0.05	8.79[31] (pK_1(NH_2))	2.6
		2.31[31] (pK_2(py-N))	
2-AEP	0.05	9.78[31] (pK_1(NH_2))	1.6
		4.24[31] (pK_2(NH_2))	
2-DMAP	0.005		21.5
	0.05		37.3*
	0.1		33.7*
	0.2		36.3*
aniline	0.02	4.65[24]	2.88*
	0.10	4.65[24]	2.88*

[a] $(k_0)_{app}$ is the measured pseudo-first-order rate constant for the combined decompositions of $C_6H_5CH(CH_3)$–$Co(DH)_2B$ and $C_6H_5CH(CH_3)$–$Co(DH)_2$(acetone) and approaches k_0 (designated by asterisks) at high concentrations of added B when displacement of acetone to form $C_6H_5CH(CH_3)$–$Co(DH)_2B$ is complete.

The above results demonstrate that addition of *excess* base ligand B to $C_6H_5CH(CH_3)$–$Co(DH)_2(H_2O)$ in acetone under N_2 provides a convenient method of determining the decomposition rate constant of in situ prepared $C_6H_5CH(CH_3)$–$Co(DH)_2B$ complexes that are difficult to isolate, e.g., $C_6H_5CH(CH_3)$–$Co(DH)_2$(2-CH_3-py). Values of k_0 obtained in acetone under N_2 for several such in situ prepared

(27) Phelan, P. F. Ph.D. Thesis, The University of Chicago, 1971; p 50.
(28) Wilkins, R. G. *The Study of Kinetics and Mechanism of Reactions of Transition Metal Complexes*; Allyn and Bacon: Boston, 1974; pp 43–45.
(29) For the purpose of the plots of Figure 4, the concentrations of 2-NH_2-py were corrected for the dissociation of $C_6H_5CH(CH_3)$–$Co(DH)_2$(2-NH_2-py) according to Scheme I.
(30) Sun, M. S.; Brewer, D. G. *Can. J. Chem.* **1967**, *45*, 2729.
(31) Goeminne, A. M.; Eeckhart, Z. *Bull. Soc. Chim. Belg.* **1971**, *80*, 605.

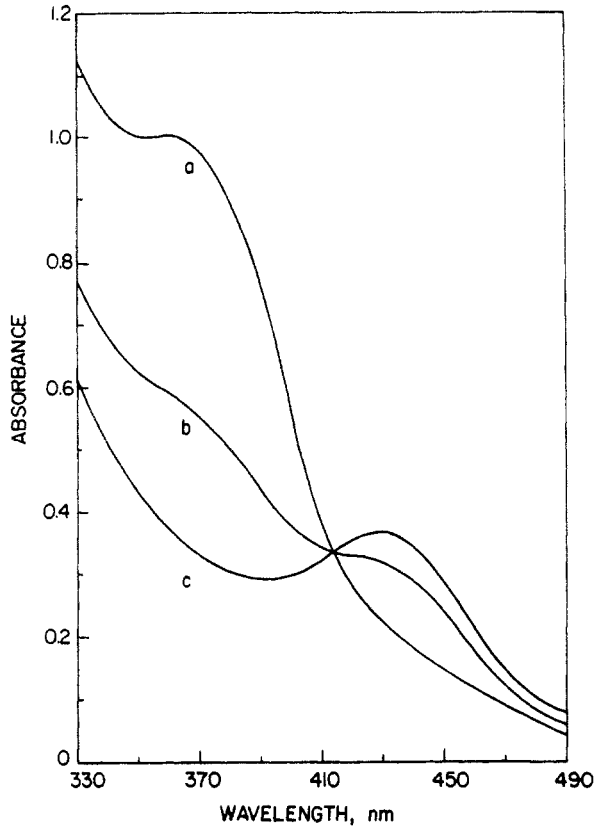

Figure 5. Spectral changes accompanying the decomposition of $C_6H_5CH(CH_3)$–$Co(DH)_2py$ (1) (initially 1.05×10^{-4} M) in toluene at 18.8 °C (cell path length 1 cm): (a) initial spectrum of 1 under N_2; (b) spectrum at equilibrium under 592 mm of H_2; (c) final spectrum after decomposition under N_2 (identical with the spectrum of 1.05×10^{-4} M $Co(DH)_2B$ in toluene).

$C_6H_5CH(CH_3)$–$Co(DH)_2B$ complexes are listed in Table III (B = 2-CH_3-py, 2-(aminomethyl)pyridine (2-AMP), 2-(2-aminoethyl)pyridine (2-AEP), 2-(dimethylamino)-pyridine (2-DMAP), aniline).

Equilibrium Studies. We have previously reported that solutions of $C_6H_5CH(CH_3)$–$Co(DH)_2$(py) in toluene, equilibrated with a constant partial pressure of H_2, attain the measurable equilibrium depicted in eq 1.[14] Similarly, decomposition of $C_6H_5CH(CH_3)$–$Co(DH)_2B$ (B = 4-CN-py, py, 4-CH_3-py, 4-NH_2-py, H_2O, imidazole, 2-NH_2-py) in acetone under H_2 (ca. 1 atm) at 25 °C also resulted in attainment of such an equilibrium.[32] Removal of the H_2 atmosphere resulted in a nearly quantitative yield of $Co^{II}(DH)_2B$, as confirmed spectrophotometrically (Figure 5). Values of K_0, defined by eq 5, were calculated from

$$K_0 = \frac{[Co^{II}(DH)_2B][C_6H_5CH{=}CH_2][H_2]^{1/2}}{[C_6H_5CH(CH_3){-}Co(DH)_2B]} \quad (5)$$

the spectrophotometrically determined equilibrium concentrations of $Co^{II}(DH)_2B$ and $C_6H_5CH(CH_3)$–$Co(DH)_2B$ and are listed in Table I. Measurements of the temperature dependence of K_0 (Appendices C–E, supplementary material) yielded excellent van't Hoff plots from which the ΔH_0 and ΔS_0 values in Table I were evaluated.

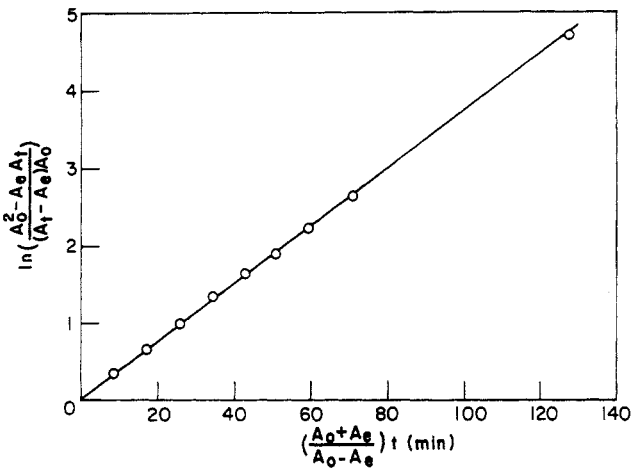

Figure 6. Decomposition of $C_6H_5CH(CH_3)$–$Co(DH)_2py$ (initially ca. 2×10^{-4} M) in toluene under 1 atm of H_2 at 24.5 °C. Kinetics of the approach to equilibrium were plotted according to eq 6.

Scheme II

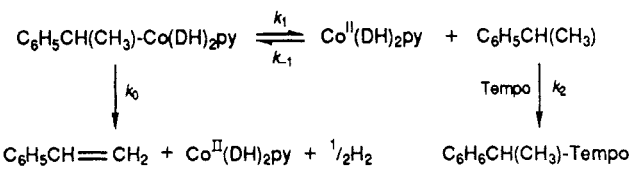

Effect of Solvent on Equilibrium Constant, K_0. Essentially identical values of K_0 for $C_6H_5CH(CH_3)$–$Co(DH)_2$(py) were obtained in toluene or acetone (Table I). This argues against an important role for solvent (acetone) coordination to the sixth coordination site of $Co^{II}(DH)_2B$ (also supported by the solvent independence of the spectra).

Kinetics of the Approach to Equilibrium. The integrated rate law for the kinetics of the approach to equilibrium is given by eq 6,[33] where A_t is the concentration of 1 at time t and A_0 and A_e are the initial and equilibrium concentrations of 1. The linear plot in Figure 6 is in

$$\ln \frac{A_0^2 - A_e A_t}{(A_t - A_e)A_0} = k_0 \frac{A_0 + A_e}{A_0 - A_e} t \quad (6)$$

accord with this and yields a k_0 value of 6.3×10^{-4} s^{-1} for $C_6H_5CH(CH_3)$–$Co(DH)_2$(py) at 24.5 °C, somewhat lower than but consistent with the k_0 value of 7.8×10^{-4} s^{-1} at 25 °C determined from the limiting rate of decomposition under N_2.

Decomposition of $C_6H_5CH(CH_3)$–$Co(DH)_2py$ in the Presence of the Free-Radical Trap Tetramethylpiperidinyl-1-oxy (Tempo, 3). In the presence of the free-radical trap Tempo (3),[34-37] an *additional* pathway of decomposition of $C_6H_5CH(CH_3)$–$Co(DH)_2py$ was observed that yielded the $C_6H_5CH(CH_3)$ radical–Tempo adduct 4 (i.e., in addition to $C_6H_5CH{=}CH_2$) according to eq 2. Yields of $C_6H_5CH(CH_3)$–Tempo were determined by ^1H NMR spectroscopy.

(32) At temperatures above 20 °C, the equilibrium corresponding to eq 1 is metastable due to slow irreversible reduction of **2**.[5,6] However, careful monitoring of the approach to "equilibrium" permitted the position of the latter to be determined with satisfactory accuracy. In some cases, the absorbance at 350–360 nm is a little higher than expected when H_2 is removed, due to the possible irreversible reduction of the dimethylglyoxime ligand. The solubilities of H_2 in toluene and acetone were obtained from: Cook, M. W.; Hanson, D. N.; Alder, B. J. *J. Chem. Phys.* **1957**, *26*, 748. Wilhelm, E.; Battino, R. *Chem. Rev.* **1973**, *73*, 1. At 25 °C, the concentrations of H_2 in acetone and toluene at 1 atm are 2.1×10^{-3} and 2.7×10^{-3} M, respectively. Concentrations of other H_2 pressures were calculated by assuming Henry's law.

(33) Frost, A. A.; Pearson, R. G. *Kinetics and Mechanism*, 2nd ed.; Wiley: New York, 1961; p 186.

(34) Root, K. S.; Hill, C. L.; Lawrence, L. M.; Whitesides, G. M. *J. Am. Chem. Soc.* **1989**, *111*, 5405.

(35) Finke, R. G.; Smith, B. L.; Mayer, B. J.; Molinero, A. A. *Inorg. Chem.* **1983**, *22*, 3677.

(36) Geno, M. K.; Halpern, J. *J. Am. Chem. Soc.* **1987**, *109*, 1238.

(37) Chateauneuf, J.; Lusztyk, J.; Ingold, K. U. *J. Org. Chem.* **1988**, *53*, 1629.

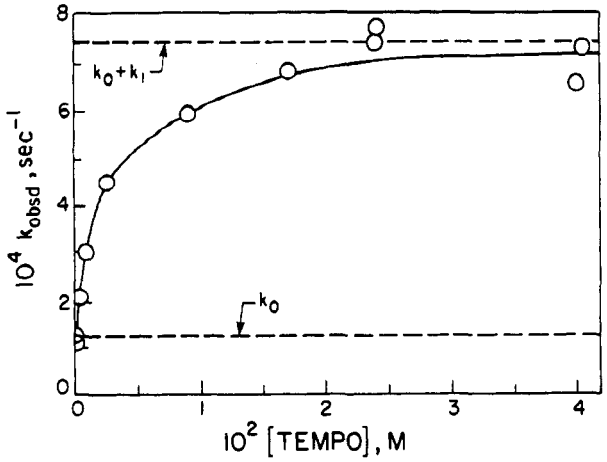

Figure 7. Dependence of k_{obsd} for the decomposition of $C_6H_5CH(CH_3)$–$Co(DH)_2py$ in acetone at 10 °C on the concentration of Tempo.

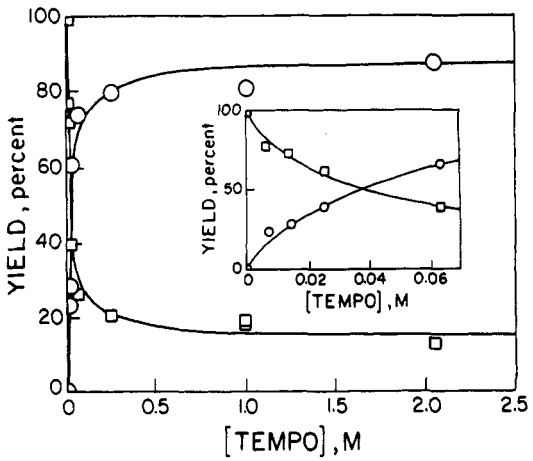

Figure 8. Dependence of the product distribution from the decomposition of $C_6H_5CH(CH_3)$–$Co(DH)_2py$ in acetone at 10 °C on the concentration of Tempo: (○) $C_6H_5CH(CH_3)$–Tempo; (□) $C_6H_5CH{=}CH_2$.

Kinetics. The kinetics of decomposition, comprising contributions from reactions 1 and 2, were monitored spectrophotometrically and found to obey the pseudo-first-order rate law

$$-d[C_6H_5CH(CH_3)\text{–}Co(DH)_2py]/dt = k_{obsd}[C_6H_5CH(CH_3)\text{–}Co(DH)_2py] \quad (7)$$

k_{obsd} and the yield of $C_6H_5CH(CH_3)$–Tempo, relative to that of $C_6H_5CH{=}CH_2$, both were found to increase with increasing Tempo concentration, reaching limiting values (7×10^{-4} s^{-1} and ca. 85:15 $C_6H_5CH(CH_3)$–Tempo:$C_6H_5CH{=}CH_2$, respectively, both at 10 °C) at $\geq 2.5 \times 10^{-2}$ M Tempo (Appendices F and and G (supplementary material); Figures 7 and 8). The results can be accommodated by Scheme II. According to this scheme

$$k_{obsd} = k_0 + \frac{k_1k_2[\text{Tempo}]}{k_{-1}[Co^{II}(DH)_2py] + k_2[\text{Tempo}]} \quad (8)$$

and

$$\frac{[C_6H_5CH{=}CH_2]}{[C_6H_5CH(CH_3)\text{–Tempo}]} = \frac{k_0k_{-1}[Co^{II}(DH)_2py]}{k_1k_2[\text{Tempo}]} + \frac{k_0}{k_1} \quad (9)$$

The instability of mixtures of $Co^{II}(DH)_2py$ and Tempo in acetone precluded the quantitative testing of the full relations of eqs 8 and 9 by simultaneous variation of the concentrations of added $Co^{II}(DH)_2py$ and Tempo. However, the data in Figures 7 and 8 clearly are in qualitative accord with these equations and with the inverse linear dependence of the ratio $[C_6H_5CH{=}CH_2]/[C_6H_5CH(CH_3)\text{–Tempo}]$ on $[\text{Tempo}]^{-1}$ depicted in Figure 9.

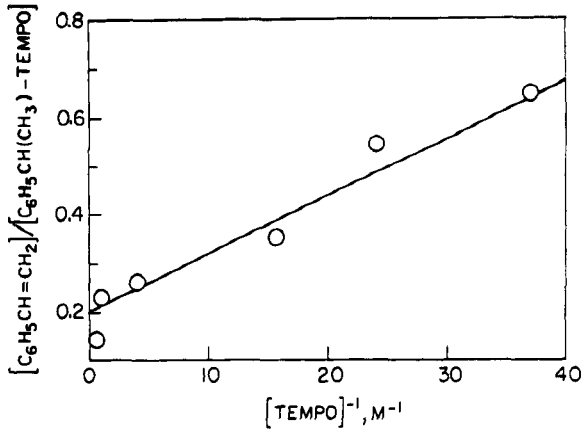

Figure 9. Dependence of the product ratio from the decomposition of $C_6H_5CH(CH_3)$–$Co(DH)_2py$ in acetone at 10 °C on the concentration of Tempo. (Data for experiments in which $[\text{Tempo}]_{initial} \leq [C_6H_5CH(CH_3)\text{–}Co(DH)_2py]_{initial}$ are omitted since [Tempo] varies significantly during the course of the reaction.)

Table IV. Comparison of k_1 Values Determined from Product Distributions and from Kinetic Measurements According to Eqs 10 and 11

temp, °C	10^4k_1(product), s^{-1}	10^4k_1(kinetic), s^{-1}
7.5	3.95	3.90
9.9	6.20	6.20
10.1	6.45	6.55
12.5	9.4	9.6
15.1	13.4	13.8
17.2	16.4	16.6
19.8	25.9	26.8
22.0	29.1	29.2
23.0	34.9	35.5
25.8	52.0	53.4
$\Delta H^{\ddagger}$, kcal mol^{-1}	22.3 ± 0.5	22.6 ± 0.6
$\Delta S^{\ddagger}$, cal mol^{-1} K^{-1}	6 ± 2	7 ± 2

In the limit of high Tempo concentrations, eqs 8 and 9 reduce to eqs 10 and 11, respectively.

$$(k_{obsd})_{lim} = k_0 + k_1 \quad (10)$$

$$\left(\frac{[C_6H_5CH{=}CH_2]}{[C_6H_5CH(CH_3)\text{–Tempo}]}\right)_{lim} = \frac{k_0}{k_1} \quad (11)$$

When the value of k_0 determined from kinetic measurements on the decomposition of $C_6H_5CH(CH_3)$–$Co(DH)_2py$ in the absence of added Tempo is used, k_1 may be determined independently from the limiting values of k_{obsd} and of $[C_6H_5CH{=}CH_2]/[C_6H_5CH(CH_3)\text{–Tempo}]$ at high Tempo concentrations, by means of eqs 10 and 11, respectively. The results of these determinations, over the temperature range 7.5–25.8 °C, are listed in Table IV and display consistently excellent agreement between the two independently determined values of k_1. The corresponding values of $\Delta H^{\ddagger}_1$ and $\Delta S^{\ddagger}_1$ are virtually identical: 22.3 ± 0.5 vs 22.6 ± 0.6 kcal mol^{-1} and 6 ± 2 vs 7 ± 2 cal mol^{-1} K^{-1}, respectively.

An *approximate* value of k_{-1}/k_2 may be deduced by fitting the plot of Figure 9 to eq 9, using for $[Co^{II}(DH)_2py]$ its average value during the reaction, i.e., $[C_6H_5CH(CH_3)\text{–}Co(DH)_2py]_{initial}/2$. This yields $k_{-1}/k_2 \approx 12$. Using the independently determined value of $k_2 = 1.6 \times 10^8$ M^{-1} s^{-1} [37] yields ca. 2×10^9 M^{-1} s^{-1}, a value close to the diffusion-controlled limit, for k_{-1}, the rate constant of recombination of the $C_6H_5CH(CH_3)$ radical with $Co^{II}(DH)_2py$.

Scheme III

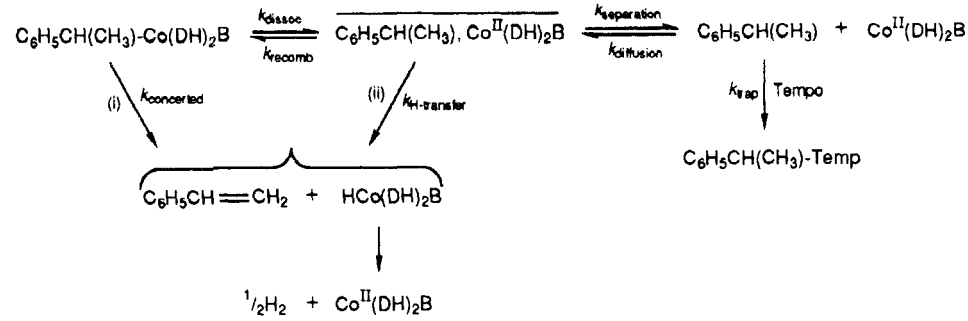

Rate constants close to the diffusion-controlled limit also have been determined for the combination of a large number of other metal radical–organic radical pairs.[38]

Discussion

Mechanism of Olefin Formation. Two possible mechanisms, encompassed by Scheme III, have previously been considered for these and related olefin-forming decomposition reactions of cobalt alkyl compounds,[3,7,8,14,15,17-21,39,40] namely (i) concerted olefin elimination and (ii) β-hydrogen atom transfer between the geminate $\overline{C_6H_5C^{\bullet}H(CH_3),Co^{II}(DH)_2py}$ radical pair that is formed by homolysis of the Co–C bond. In both cases, H_2 is formed from an intermediate $HCo(DH)_2B$ complex. Support for such an intermediate has been provided by trapping with phenylacetylene,[41] and evolution of H_2 from an $HCo(DH)_2B$ complex has been directly observed.[42]

According to (i)

$$k_0 = k_{\text{concerted}} \tag{12}$$

$$k_1 = \frac{k_{\text{dissoc}}k_{\text{separation}}}{k_{\text{recomb}} + k_{\text{separation}}} \tag{13}$$

On the other hand, according to (ii)

$$k_0 = \frac{k_{\text{dissoc}}k_{\text{H-transfer}}}{k_{\text{recomb}} + k_{\text{H-transfer}} + k_{\text{separation}}} \tag{14}$$

$$k_1 = \frac{k_{\text{dissoc}}k_{\text{separation}}}{k_{\text{recomb}} + k_{\text{H-transfer}} + k_{\text{separation}}} \tag{15}$$

We first proposed alternative ii for reaction 1[14,15] and for the closely related decompositions of R-Co(Saloph)py (Saloph = *N,N'*-bis(salicylidene)-*o*-phenylenediamine, R = $CH_3CH_2CH_2$, $(CH_3)_2CH$).[39] Subsequently, this interpretation has been extended by us to the decomposition of cyclopentylmethylcobalamin[40] and adopted by others for several related systems.[19-21] We continue to favor it for the present system and cite the following evidence in support.

(1) The vacant cis-coordination site that usually is considered a requirement for concerted olefin elimination[43] is not readily accessible in these six-coordinate 18-electron complexes.

Table V. Comparison of Activation Parameters (kcal mol^{-1}) for Olefin- and Free-Radical-Forming Reactions of Various Alkylcobalt Compounds

	olefin formation		free-radical formation		
cobalt alkyl	$\Delta H^{\ddagger}$	$\Delta G^{\ddagger}$ (25 °C)	$\Delta H^{\ddagger}$	$\Delta G^{\ddagger}$ (25 °C)	ref
$C_6H_5CH(CH_3)$–Co(DH)$_2$py	21.6	22.2	22.4	20.6	this work
$CH_3CH_2CH_2$–Co(Saloph)py	23.4	27.9	27.1	26.2	39
$(CH_3)_2CH$–Co(Saloph)py	19.8	24.6	21.8	22.7	39
cyclo-$C_5H_9CH_2$–cobalamin	25.3	26.5	25.2	26.1	40

(2) Competition between β-hydrogen abstraction and cage separation has been demonstrated by CIDNP for a related geminate radical pair (eq 16).[44] Facile β-H atom

$$C_6H_5C(CH_3)=CH_2 + HMn(CO)_5 \rightleftharpoons \overline{C_6H_5\dot{C}(CH_3)_2,\dot{M}n(CO)_5} \rightarrow C_6H_5\dot{C}(CH_3)_2 + \dot{M}n(CO)_5 \tag{16}$$

transfer from alkyl radicals to other cobalt(II) complexes also has been observed (eq 17).[45]

$$RCH_2\dot{C}H_2 + Co(CN)_5^{3-} \rightarrow RCH=CH_2 + HCo(CN)_5^{3-} \tag{17}$$

(3) Involvement of a geminate radical pair intermediate has been deduced from the stereoselectivities, kinetic isotope effects, and substituent effects in the olefin-forming decompositions of various phenylalkyl–Co(DH)$_2$py complexes.[19,20] An earlier proposal[8] of a nonradical concerted pathway for such reactions has been retracted,[19] although it has been suggested that there is some contribution from such a pathway for related *acid-catalyzed* decompositions in *aqueous solutions*.[18]

(4) The closely related activation parameters of the olefin-forming and free-radical-trapping reactions (eqs 1 and 2, respectively) suggest that both proceed through the same rate-determining step, viz. Co–C bond homolysis to generate a geminate radical pair according to scheme III, path ii. This close correspondence between the activation parameters of free-radical formation and olefin elimination now has been observed for several other organocobalt compounds (Table V), suggesting that in these cases also, olefin elimination proceeds through Co–C bond homolysis.

(5) Photolysis of an acetone solution of $C_6H_5CH(CH_3)$–Co(DH)$_2$py in the presence of 1 M Tempo yields a product distribution (ca. 10% $C_6H_5CH=CH_2$, 90% $C_6H_5CH(CH_3)$–Tempo) similar to that from thermolysis.[23] Since photolysis almost certainly induces homolytic Co–C

(38) Halpern, J. *ACS Symp. Ser.* **1990**, *428*, 100.
(39) Tsou, T. T.; Loots, M.; Halpern, J. *J. Am. Chem. Soc.* **1982**, *104*, 623.
(40) Kim, S. H.; Chen, H. L.; Feilchenfeld, N.; Halpern, J. *J. Am. Chem. Soc.* **1988**, *110*, 3120.
(41) Naumberg, M.; Duong, K. V. N.; Gaudemer, A. *J. Organomet. Chem.* **1970**, *25*, 231.
(42) Chao, T. H.; Espenson, J. H. *J. Am. Chem. Soc.* **1978**, *100*, 129.
(43) Collman, J. P.; Hegedus, L. S.; Norton, J. R.; Finke, R. G. *Principles and Applications of Transition Metal Chemistry*, 2nd ed.; University Science Publishers: Mill Valley CA, 1987; p 386.
(44) Sweany, R. L.; Halpern, J. *J. Am. Chem. Soc.* **1977**, *99*, 8335.
(45) Halpern, J. *Pure Appl. Chem.* **1979**, *51*, 2171 and references therein.

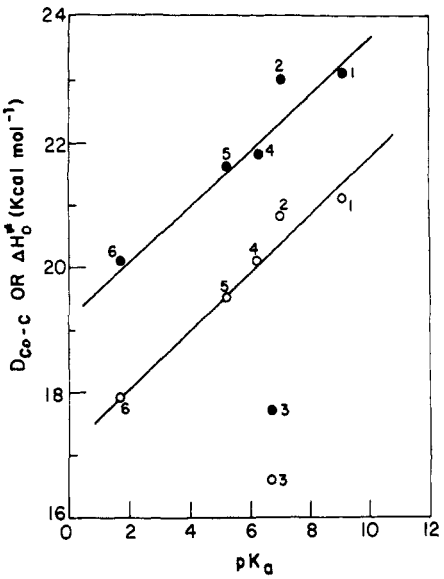

Figure 10. Variation of D_{Co-C} and $\Delta H_0^{\ddagger}$ with the pK_a of B for the decomposition of $C_6H_5CH(CH_3)$–$Co(DH)_2B$ in acetone: (1) 4-NH_2-py; (2) imidazole; (3) 2-NH_2-py; (4) 4-CH_3-py; (5) py; (6) 4-CN-py; (●) $\Delta H_0^{\ddagger}$; (○) D_{Co-C}.

bond dissociation *with initial formation* of a geminate $C_6H_5C^{\bullet}(CH_3),Co^{II}(DH)_2py$ radical pair,[46] this result suggests that olefin formation during thermolysis also proceeds through this path.

Thus, there is a diverse and persuasive body of evidence for the conclusion that olefin formation in reaction 1 proceeds by H-atom transfer between a geminate radical pair generated by Co–C bond homolysis.

Deduction of the Co–C Bond Dissociation Energy (BDE) from Kinetic Measurements on Reaction 2. The Co–C bond dissociation energy (D_{Co-C}, strictly bond dissociation *enthalpy*) of $C_6H_5CH(CH_3)$–$Co(DH)_2py$ may be deduced from measurements of the kinetics of the bond dissociation process (eq 18) through the relation of eq 19.

$$C_6H_5CH(CH_3)\text{–}Co(DH)_2py \underset{k_{-1}}{\overset{k_1}{\rightleftharpoons}} Co^{II}(DH)_2py + C_6H_5\dot{C}H(CH_3) \left(\xrightarrow{\text{Tempo}} C_6H_5CH(CH_3)\text{–Tempo}\right) \quad (18)$$

$$\Delta H_1 = \Delta H^{\ddagger}_1 - \Delta H^{\ddagger}_{-1} \approx D_{Co-C} \quad (19)$$

This approach, which we introduced in 1982,[39] has since been used extensively for measuring transition-metal–alkyl (especially cobalt–alkyl) bond dissociation energies,[16,35,36,40,47-51] and its validity now is well established.[38,52] Where, as in the present case, the rate of the Co–C bond-forming reaction is close to the diffusion-controlled rate ($k_{-1} \approx 2 \times 10^9$ M^{-1} s^{-1}), $\Delta H^{\ddagger}_{-1}$ can be approximated by the activation enthalpy for viscous flow, namely 2 ± 1 kcal mol^{-1} for acetone and other common solvents of low viscosity.[53] Thus, $D_{Co-C} \approx \Delta H^{\ddagger}_1 - 2$ kcal mol^{-1}. Using the previously determined value of 22.4 kcal mol^{-1} for $\Delta H^{\ddagger}_1$ yields 20.4 ± 1.2 kcal mol^{-1} for the Co–C BDE of $C_6H_5CH(CH_3)$–$Co(DH)_2py$.

The applications and limitations of this procedure have recently been reviewed.[38,52,54] Confirmation of its validity in a system closely related to the present one is provided by the excellent agreement the Co–C BDE's of $C_6H_5CH_2$–$Co(DH)_2py$ determined by this method[55] and, independently, from calorimetric measurements[56] (29 vs 31 kcal mol^{-1}, each ca. ± 2 kcal mol^{-1}, respectively).

Deduction of the Co–C Bond Dissociation Energy from Measurements of the Equilibrium Constants of Reaction 1. The Co–C bond dissociation energy of $C_6H_5CH(CH_3)$–$Co(DH)_2py$ also may be deduced from ΔH_0 of reaction 1, derived from measurements of the temperature dependence of the equilibrium constant, K_0, through the thermodynamic cycle of eqs 20–22.

$$C_6H_5CH(CH_3)\text{–}Co(DH)_2py \rightleftharpoons C_6H_5CH{=}CH_2 + Co^{II}(DH)_2py + \tfrac{1}{2}H_2 \quad \Delta H \text{ vs } \Delta H_0 \quad (20)$$

$$C_6H_5CH{=}CH_2 + \tfrac{1}{2}H_2 \rightleftharpoons C_6H_5\dot{C}H(CH_3) \quad \Delta H_{21} \quad (21)$$

$$C_6H_5CH(CH_3)\text{–}Co(DH)_2py \rightleftharpoons C_6H_5\dot{C}H(CH_3) + Co^{II}(DH)_2py \quad D_{Co-C} \quad (22)$$

Thus

$$D_{Co-C} = \Delta H_0 + \Delta H_{21} \quad (23)$$

$$= \Delta H_0 + \Delta H_f(C_6H_5\dot{C}H(CH_3)) - \Delta H_f(C_6H_5CH{=}CH_2) \quad (24)$$

where ΔH_f is the enthalpy of formation of the designated species. Substituting the previously determined value of 22.1 kcal mol^{-1} for ΔH_0 and the literature value[57] of 35.2 kcal mol^{-1} for the enthalpy of formation of $C_6H_5CH{=}CH_2$ yields

$$D_{Co-C} = \Delta H_f(C_6H_5\dot{C}H(CH_3)) - 13.1 \text{ kcal mol}^{-1} \quad (25)$$

Prior to 1981, the accepted literature value of the enthalpy of formation of the $C_6H_5\dot{C}H(CH_3)$ radical was 33 kcal mol^{-1}.[58] Using this value yields 19.9 kcal mol^{-1} for D_{Co-C}, in excellent agreement with the value of 20.4 kcal mol^{-1} deduced above by a totally independent route from measurements of $\Delta H^{\ddagger}_1$.

A more recent determination has yielded a significantly higher value of 39.6 kcal mol^{-1} for the enthalpy of formation of the $C_6H_5\dot{C}H(CH_3)$ radical.[59] Substituting this value into eq 25 yields a value of 26.5 kcal mol^{-1} for the Co–C BDE of $C_6H_5CH(CH_3)$–$Co(DH)_2py$. Since D_{Co-C} ($\sim\Delta H_1$) *must* be lower than $\Delta H^{\ddagger}_1$, this is incompatible with the experimentally determined value of 22.4 kcal mol^{-1} for $\Delta H^{\ddagger}_1$. Thus, we favor the lower value of 33 kcal mol^{-1} for $\Delta H_f(C_6H_5\dot{C}H(CH_3))$ and, indeed, our measurements of D_{Co-C} lead to the independent deduction of this value via the thermodynamic cycle of eqs 20–22.[60]

A possible explanation of this discrepancy may be provided by solvent effects, since our measurements are in acetone solution whereas the literature data for the heats of formation of $C_6H_5CH(CH_3)$ refer to the gas phase.

(46) Toscano, P. J.; Marzilli, L. G. *Prog. Inorg. Chem.* **1984**, *31*, 105.
(47) (a) Finke, R. G.; Hay, B. P. *Inorg. Chem.* **1984**, *23*, 3041. (b) Finke, R. G.; Hay, B. P. *J. Am. Chem. Soc.* **1986**, *108*, 4820.
(48) Halpern, J.; Kim, S. H.; Leung, T. W. *J. Am. Chem. Soc.* **1984**, *106*, 8317.
(49) Collman, J. P.; McElwee-White, L.; Brothers, P. J.; Rose, E. *J. Am. Chem. Soc.* **1986**, *108*, 1332.
(50) Bakac, A.; Espenson, J. H. *J. Am. Chem. Soc.* **1984**, *106*, 5197.
(51) Martin, B. D.; Finke, R. G. *J. Am. Chem. Soc.* **1990**, *112*, 2419.
(52) Halpern, J. *Polyhedron* **1988**, *7*, 1483.
(53) Visanath, D. S.; Natarajan, G. *Data Book on the Viscosity of Liquids*; Hemisphere Publishing: New York, 1989.
(54) Koenig, T. W.; Hay, B. P.; Finke, R. G. *Polyhedron* **1988**, *7*, 1499.
(55) Geno, M.; Halpern, J. Unpublished results.
(56) Toscano, P. J.; Seligson, A. L.; Curran, M. T.; Skorobutt, A. J.; Sonnenberger, D. C. *Inorg. Chem.* **1987**, *28*, 166.
(57) Stull, D. R.; Westrum, E. F.; Sinke, G. C. *The Chemical Thermodynamics of Organic Compounds*; Wiley: New York, 1969.
(58) Kerr, J. A. *Chem. Rev.* **1966**, *66*, 465.
(59) Robaugh, D. A.; Stein, S. E. *J. Chem. Kinet.* **1984**, *13*, 445.
(60) This has implications also for the values of the $C_6H_5C(CH_3)$–H and $C_6H_5CH(CH_3)$–CH_3 bond dissociation energies.[59,61]
(61) McMillen, D. F.; Golden, D. M. *Annu. Rev. Phys. Chem.* **1982**, *33*, 493.

However, solvent effects on reactions such as (1) and (2) that involve neutral species are expected to be small, and this is supported by the invariance of ΔH_0 and $\Delta H^{\ddagger}_0$ on going from acetone to toluene.

Dependence of D_{Co-C} on B for 4-Substituted Pyridines. Values of D_{Co-C} for the various $C_6H_5CH(CH_3)$-$Co(DH)_2B$ compounds, deduced from the measured values of ΔH_0 by means of eq 24 (with use of 33 kcal mol^{-1} for $\Delta H_f(C_6H_5\dot{C}H(CH_3))$, are listed in Table I. Because they constitute a sterically invariant series, the 4-substituted pyridines are appropriate for the examination of the influence of electronic factors on the Co–C bond dissociation energy. For this series, as depicted in Figure 10, D_{Co-C} was found to increase linearly with the pK_a of B. This trend previously has been interpreted[15] in terms of the decrease in oxidation state of cobalt (i.e., $Co^{III} \rightarrow Co^{II}$) that accompanies homolytic Co–C bond dissociation (eq 22). Thus, more basic ligands are expected to stabilize the higher oxidation state, i.e., the organocobalt compound and, accordingly, to increase the barrier to homolytic dissociation. The value of D_{Co-C} for B = imidazole also is seen to lie close to the same plot.

Relation between $\Delta H_0^{\ddagger}$ and D_{Co-C} for 4-Substituted Pyridines. Figure 10 reveals that the dependence of $\Delta H^{\ddagger}_0$ on pK_a for the 4-substituted pyridine series (and imidazole) closely parallels that of D_{Co-C}, the difference between $\Delta H^{\ddagger}_0$ and D_{Co-C} having a constant value of ca. 2 kcal mol^{-1}. This is consistent with our earlier suggestion that reaction 1 is initiated by a rate-determining homolysis of the Co–C bond, followed by β-hydrogen transfer from the C_6H_5CH-CH_3 radical to $Co^{II}(DH)_2py$ and decomposition of the resulting cobalt hydride in accord with Scheme III, path ii.

The small difference (ca. 2 kcal mol^{-1}) between $\Delta H^{\ddagger}_0$ and ΔH_0 implies that the activation enthalpy for the reverse reaction of eq 1 is very small. This is consistent with a reported value of ca. 3 kcal mol^{-1} for $\Delta H^{\ddagger}$ of the reaction of $Co^{II}(DH)_2py$ with H_2 and $C_6H_5CH{=}CH_2$ in methanol[5] and with reported values of $\Delta H^{\ddagger} \approx 0$ and $\Delta H = -11$ kcal mol^{-1} for the reaction $2Co^{II}(CN)_5^{3-} + H_2 \rightarrow 2HCo(CN)_5^{3-}$.[62,63] Considerations of microscopic reversibility (Scheme III, path ii) suggest that the reverse of reaction 1 proceeds by the sequence of eqs 26 and 27, in which $\Delta H^{\ddagger}$ of the rate-determining step (eq 27) is expected to be offset by an exothermic preequilibrium (eq 26) so that the overall apparent $\Delta H^{\ddagger}$ is small.

$$2Co^{II}(DH)_2B + H_2 \rightleftharpoons 2HCo(DH)_2B \quad (26)$$

$$HCo(DH)_2B + C_6H_5CH{=}CH_2 \rightarrow C_6H_5C^{\cdot}H(CH_3),Co^{II}(DH)_2B \quad (27)$$

2-Substituted Pyridines [B = 2-NH_2-py, 2-NH_2CH_2-py (2-AMP), 2-$NH_2CH_2CH_2$-py (2-AEP), 2-CH_3-py] and Aniline. With the exception of 2-NH_2-py, for which the thermodynamics and kinetics of reaction 1 were fully elucidated, the study of these systems was confined to determination of k_0 at 25 °C (Table III). The previously demonstrated correlation between $\Delta H^{\ddagger}_0$ (hence, implicitly, k_0) and D_{Co-C} for the 4-substituted pyridine and imidazole systems suggests that comparisons of k_0 might reflect, at least qualitatively, corresponding trends of the Co–C bond dissociation energies. For the purpose of such comparisons, values of log k_0 for all the systems studied are plotted against the pK_a of B in Figure 11.

The linear plot in Figure 11, drawn through the points for the sterically invariant 4-substituted pyridines, reflects

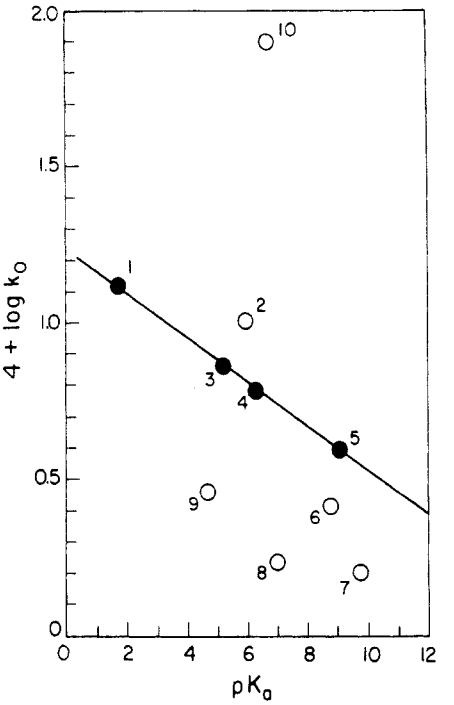

Figure 11. Dependence of log k_0 at 25 °C on pK_a of B: (1) 4-CH_3-py; (2) 2-CH_3-py; (3) py; (4) 4-CH_3-py; (5) 4-NH_2-py; (6) 2-AMP; (7) 2-AEP; (8) imidazole; (9) aniline; (10) 2-NH_2-py.

the influence of the basicity of B on the Co–C bond dissociation energies in the absence of steric influences. In view of the marked dependence of k_0 on the steric influence of B, found earlier for a series of phosphine ligands,[16] the variation of k_0 among these complexes seems rather small, although in the expected direction. Thus, for a series of B ligands with similar pK_a's (ca. 6), k_0 decreases along the sequence 2-CH_3-py > 4-CH_3-py > imidazole, which also is the order of decreasing steric bulk. Complexes of the three primary amines (aniline, 2-AMP, and 2-AEP) also exhibit an inverse dependence of k_0 on pK_a but with values consistently lower than those for the sterically more demanding pyridine ligands. The largest enhancement of k_0 (and correspondingly lowest value of $\Delta H^{\ddagger}_0$) are observed for 2-NH_2-py. This is difficult to accommodate on steric grounds alone, since 2-NH_2-py is expected to be sterically comparable to or less demanding than 2-CH_3-py.[64] An explanation may be provided by the results of earlier X-ray structural and NMR studies on related R-$Co(DH)_2$(2-NH_2-py) complexes.[65,66] These studies reveal that, in the solid state, 2-NH_2-py is coordinated to the Co atom of *i*-Pr-$Co(DH)_2$(2-NH_2-py) through the endocyclic pyridine nitrogen. This also was found to be the predominant form in solution, although equilibration, through an intramolecular isomerization, with the exocyclic NH_2-coordinated isomer (ca. 17% in the case of *i*-Pr-$Co(DH)_2$(2-NH_2-py)) could be detected. The measured value of $k_{2\text{-}NH_2\text{-}py}$ presumably refers to the predominant endo-bound isomer (which, on steric grounds, is expected to be more reactive than the exo isomer; cf. the pyridine and aniline complexes). For the endo isomer of *i*-Pr-$Co(DH)_2$(2-NH_2-py), the X-ray structure reveals an abnormally long Co–N bond (2.194 Å, compared with 2.099 Å for the Co–N bond of

(62) DeVries, B. *J. Catal.* **1962**, *1*, 489.
(63) Halpern, J.; Pribanic, M. *Inorg. Chem.* **1970**, *9*, 2616.
(64) Hirsch, J. A. *Top. Stereochem.* **1967**, *1*, 199.
(65) Summers, M. F.; Toscano, P. J.; Bresciani-Pahor, N.; Nardin, G.; Randaccio, L.; Marzilli, L. G. *J. Am. Chem. Soc.* **1983**, *105*, 6259 and references therein.
(66) Marzilli, L. G.; Summers, M. F.; Zangrando, E.; Bresciani-Pahor, N.; Randaccio, L. *J. Am. Chem. Soc.* **1986**, *108*, 4830 and references therein.

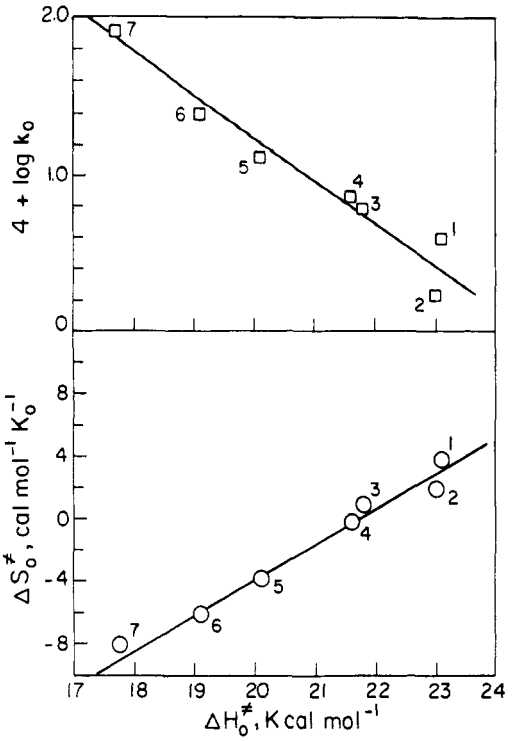

Figure 12. Dependence of $\Delta S_0^{\ddagger}$ (○) and log k_0 (□) at 25 °C on $\Delta H_0^{\ddagger}$: (1) 4-NH_2-py; (2) imidazole; (3) 4-CH_3-py; (4) py; (5) 4-CN-py; (6) acetone; (7) 2-NH_2-py.

i-Pr-Co(DH)$_2$(py)) possibly associated with a distortion induced by H-bonding between the NH_2 groups and an oxygen atom of the dimethylglyoxime ligand.[65] Such a lengthening of the trans-Co–N bond (making 2-NH_2-py a poorer electron donor) would be expected to weaken the Co–C bond[65] and, hence, to increase its rate of dissociation (i.e., k_0).

Compensation Effects in the Activation Parameters for Co–C Bond Dissociation. We have recently drawn attention to the observation of a recurrent pattern of systematic partial "compensation" of the activation parameters for the homolytic Co–C bond dissociation reactions of series of closely related organocobalt compounds, such that $\Delta S^{\ddagger}_0$ becomes increasingly positive as $\Delta H^{\ddagger}_0$ increases.[52,67] Figure 12 reveals that the data of Table I also exhibit such a trend, which extends not only to the 4-substituted pyridine and imidazole derivatives but also to those for which B = 2-NH_2-py and acetone. There are well-recognized grounds for treating such "compensation effects" with suspicion, since they commonly have an artifactual origin reflecting the interdependence of $\Delta H^{\ddagger}_0$ and $\Delta S^{\ddagger}_0$.[68] However, careful examination of these trends, with use of a variety of criteria, has led us to conclude that they are indeed genuine and reflect a systematic dependence of the structural features of the transition state on $\Delta H^{\ddagger}_0$. The bond dissociation process associated with $\Delta H^{\ddagger}_0$ is substantially endothermic, and the activation barrier associated with the reverse (recombination) reaction is small. Thus, the transition state for the dissociation is anticipated to be "product-like" and to become more so with increasing endothermicity (i.e., with increasing D_{Co-R} and $\Delta H^{\ddagger}_0$ (Hammond principle)).[69] Since the entropy of the overall dissociation process is substantially positive, it is expected that this should be accompanied by an increase in $\Delta S^{\ddagger}_0$ possibly associated with increasing relaxation of the original rigid octahedral configuration.

The systematic dependence of $\Delta S^{\ddagger}_0$ on $\Delta H^{\ddagger}_0$ also implies a systematic dependence of k_0 and $\Delta H^{\ddagger}_0$, which also is depicted in Figure 12. This supports our earlier use of k_0 as a rough measure of relative Co–C bond dissociation energies.[16]

Experimental Section

Materials. High-purity N_2, Ar, or H_2 (Linde) was passed through a catalytic deoxygenation purifier prior to use. 4-Aminopyridine, 4-methylpyridine, 4-cyanopyridine, imidazole, 2-aminopyridine, 2-(aminomethyl)pyridine, 2-(2-aminoethyl)-pyridine, 2-(dimethylamino)pyridine, aniline, dimethylglyoxime, and cobalt acetate were obtained from Aldrich. 2-Methylpyridine was obtained from BDH. Reagent-grade pyridine was obtained from Baker. Toluene (Baker) was distilled and stored over 5A molecular sieves. Acetone (Baker) was distilled from a twice-crystallized NaI·$(CH_3)_2CO$ adduct, purged with N_2, and subjected to four pump (10^{-2} Torr)/fill (N_2) cycles. Acetone-d_6 was degassed with N_2. Styrene was stirred over ferrous sulfate and freshly vacuum-distilled prior to use in the equilibrium studies. Most of the pyridine and imidazole type ligands were purified by recrystallization or distillation prior to use. Tempo (Aldrich) was sublimed and degassed with N_2.

$C_6H_5CH(CH_3)$–Co(DH)$_2$B complexes were prepared by literature procedures.[3] In a typical preparation, 1.85 g of dimethylglyoxime was stirred in ~30 mL of methanol under N_2. About 2 g of cobalt acetate was added, and the solution turned brown with some brown precipitate. Approximately 1 mL of styrene was added to the solution under N_2. Subsequently, H_2 was bubbled through the solution (~2–3 h) at room temperature in the dark until a homogeneous brown solution was obtained. Addition of the base ligand (B:Co = 1:1) resulted in a brown precipitate of $C_6H_5CH(CH_3)$–Co(DH)$_2$B (B = 4-CN-py, 4-NH_2-py, py, 4-CH_3-py, imidazole). For $C_6H_5CH(CH_3)$–Co(DH)$_2$B (where B = H_2O, 2-NH_2-py), the product precipitated only when the solution was cooled in a dry ice/acetone bath. Rapid filtration of the complexes in the dark is required to minimize the decomposition of the $C_6H_5CH(CH_3)$–Co(DH)$_2$B complexes. The dried $C_6H_5CH(CH_3)$–Co(DH)$_2$B complexes, characterized by low-temperature NMR spectroscopy, may be kept in aluminum-foil-wrapped vials in the cold for weeks. The λ_{max} and ϵ values for the visible absorption spectra of the complexes are listed in Appendix H (supplementary material). The NMR data for the complexes, determined with a Bruker 80-MHz (University of Waterloo Chemistry Department) or a Bruker 270-MHz spectrometer (University of Chicago Chemistry Department), are listed in Appendix I (supplementary material).

$C_6H_5CH(CH_3)$–Co(DH)$_2$B (B = 2-(aminomethyl)pyridine, 2-(2-aminoethyl)pyridine, 2-(dimethylamino)pyridine, and 2-CH_3-py) were prepared in situ by addition of excess base ligand, B, to $C_6H_5CH(CH_3)$–Co(DH)$_2$(H_2O) in acetone under N_2.

Co^{II}(DH)$_2$B complexes were prepared by literature procedures[70] and stored under an oxygen-free atmosphere. Spectral data are listed in Appendix J (supplementary material).

$C_6H_5CH(CH_3)$–Tempo. Preparation of the $C_6H_5CH(CH_3)$ Grignard reagent in the presence of Tempo yielded 1-(phenylethoxy)-2,2,6,6-tetramethylpiperidine, $C_6H_5CH(CH_3)$–Tempo, as the major product.[34] A 4-mL diethyl ether solution of 1-(bromoethyl)benzene (0.32 mL, 2.3 mmol) and Tempo (2.0 g, 13 mmol) added to magnesium ribbon (0.072 g, 3.0 mmol) was refluxed in a flame-dried flask under N_2 for 2 h. The solvent of the resulting orange solution was removed under reduced pressure at 25 °C, and the crude product was extracted with three 20-mL portions of hexane, which was also removed by vacuum. After it was recrystallized four times from methanol to remove unreacted 1-(bromoethyl)benzene, the product was separated from solvent and unreacted Tempo by pumping overnight at 0.01 Torr. ^{1}H NMR (C_6D_6): δ 7.44–6.86 (m, 5 H, phenyl H), 4.84 (q, 1 H, benzylic

(67) Halpern, J. *Bull. Chem. Soc. Jpn.* **1988**, *61*, 13 and references therein.
(68) (a) Leffler, J. E. *J. Org. Chem.* **1955**, *20*, 1202. (b) Peterson, R. C. *J. Org. Chem.* **1964**, *29*, 3133. (c) Exner, O. *Prog. Phys. Org. Chem.* **1973**, *10*, 411.
(69) Hammond, G. S. *J. Am. Chem. Soc.* **1955**, *77*, 334.
(70) Schneider, P. W.; Phelan, P. F.; Halpern, J. *J. Am. Chem. Soc.* **1969**, *91*, 77.

H), 1.48 (d, 3 H, Me H), 1.34, 1.23, 1.11, 0.80 (4 s, 18 H, Tempo H). $^{13}C\{^1H\}$ NMR (C_6D_6): ∂ 127.3, 127.1, 146.1, 83.7, 59.9 (d), 40.7, 34.7 (d), 23.6, 20.6, 17.6. MS (CI+, propane): 262 (72, M + H), 158 (86, Tempo + H_2), 157 (86, Tempanol + H), 156 (61, Tempo), 142 (36, Tempo - Me), 140 (78), 126 (13). Anal. Found (calcd): C, 75.89 (78.11); H, 10.23 (10.41); N, 5.21 (5.36). Mp (sealed capillary): 42–43 °C.

Kinetic Measurements. $C_6H_5CH(CH_3)$–$Co(DH)_2B$ and Tempo were dissolved in the thermostated solvent (toluene or acetone) in the complete absence of oxygen and transferred to a thermostated spectrophotometric cell that was sealed off from the atmosphere with a Roto-seal tap (Kontes). Most of the kinetic measurements were made in a Cary 219 or Perkin-Elmer Lambda 3 spectrophotometer equipped with a thermostated cell block. The rates were measured by monitoring the absorbance changes at 430–460 nm. Values of k_0 were obtained from the slopes of plots of log $|A_\infty - A_t|$ vs time at 430–460 nm or log $|A_t - A_\infty|$ vs time at 350–360 nm.

Equilibrium Studies. The procedure for the equilibrium measurements was similar to that for the kinetic studies. However, $C_6H_5CH(CH_3)$–$Co(DH)_2B$ was dissolved at 0 °C under H_2 and the total pressure of H_2 adjusted with a manometer. The rate of approach to equilibrium was measured by monitoring the increase in absorbance at 430–460 nm and decrease in absorbance at 350–360 nm, since catalytic reduction of $Co(DH)_2B$ by H_2 is a complicating factor above 20 °C. The equilibrium position was identified as the maximum absorbance reached at ~460 nm and the corresponding absorbance at ~350 nm. The equilibrium concentrations of $C_6H_5CH(CH_3)$–$Co(DH)_2B$ (1) and $Co^{II}(DH)_2B$ (2) were calculated (eqs 28 and 29) by using the absorbance at

$$A_e^{430} = [1]_e\epsilon_1^{430}l + [2]_e\epsilon_2^{430}l \quad (28)$$

$$A_e^{350} = [1]_e\epsilon_1^{350}l + [2]_e\epsilon_2^{350}l \quad (29)$$

two different wavelengths (430 and 350 nm) attained at equilibrium (where A_e^{430} and A_e^{350} are the equilibrium absorbances at 430 and 350 nm, respectively, ϵ_1^{430} and ϵ_1^{350} are the molar extinction coefficients of 1 at 430 and 350 nm, respectively; ϵ_2^{430} and ϵ_2^{350} are the molar extinction coefficients of 2 at 430 and 350 nm, respectively, and l is the cell path length). The wavelengths and extinction coefficiens used to calculate the equilibrium concentrations of 1 and 2 are listed in Appendices H and J. The stoichiometry for thermolysis is established according to eq 1. Thus, in the absence of added styrene, [styrene] at equilibrium equals $[2]_e$ and, hence, the equilibrium constant is given by eq 30.

$$K_0 = \frac{[2]_e^2[H_2]^{1/2}}{[1]_e} \quad (30)$$

For $C_6H_5CH(CH_3)$–$Co(DH)_2(H_2O)$ in acetone under H_2, styrene was added in order to achieve a measurable equilibrium; thus

$$K_0 = \frac{[2]_e[\text{styrene}]_T[H_2]^{1/2}}{[1]_e} \quad (31)$$

where $[\text{styrene}]_T$ = initial [styrene] + [styrene] at equilibrium = initial [styrene] + $[2]_e$.

Product Analysis. Product analyses were performed on 2×10^{-3} M $C_6H_5CH(CH_3)$–$Co(DH)_2B$ solutions after complete decomposition. The stoichiometry of H_2 evolution was confirmed in some cases, namely, $C_6H_5CH(CH_3)$–$Co(DH)_2$(py), $C_6H_5CH(CH_3)$–$Co(DH)_2$(imidazole), and $C_6H_5CH(CH_3)$–$Co(DH)_2$(4-NH_2-py), with use of a constant-pressure gas-uptake apparatus.[71] H_2 also was quantitatively identified for $C_6H_5CH(CH_3)$–$Co(DH)_2$(4-CN-py) and $C_6H_5CH(CH_3)$–$Co(DH)_2$(py) via GLC (Hewlett-Packard Model 700 chromatograph equipped with a 6-ft molecular sieve (5A) column with N_2 as carrier gas). Mass spectrometry also was used to identify the evolution of H_2 from the thermolysis of $C_6H_5CH(CH_3)$–$Co(DH)_2$(py). Styrene was identified by NMR spectroscopy or by GLC with use of a Hewlett-Packard 5750 or 5880 research model and a 6-ft 5% Carbowax 20 M column. $Co^{II}(DH)_2B$ was identified and quantified by spectral matching with authentic samples.

Products from thermolyses in the presence of Tempo were determined by ^1H NMR spectroscopy with use of the University of Chicago 500-MHz FT-NMR spectrometer. Sealed-tube NMR samples were prepared by syringe and Schlenk techniques at −80 °C in subdued light from purified deuterioacetone and weighed $C_6H_5CH(CH_3)$–$Co(DH)_2$py and Tempo. A total of 60 scans with a sweep width large enough to prevent folding over of the peaks due to paramagnetic Tempo and a delay time of 5 s to prevent saturation afforded the reproducible measurement of styrene and $C_6H_5CH(CH_3)$–Tempo peak integrals at ∂ 5.33 and 4.85 versus hexamethyldisiloxane at ∂ 0.012. A control experiment confirmed the validity of the NMR determinations up to Tempo concentrations of 2 M.

Acknowledgment. Support of this research through grants from the National Institutes of Health and the National Science Foundation of the U.S. and the Natural Sciences and Engineering Research Council of Canada is gratefully acknowledged. The NMR facilities were supported in part through The University of Chicago Cancer Center Grant No. NIH-CA-14599.

Supplementary Material Available: Appendices A–J, listings of rate constants, equilibrium constants, and spectroscopic data for individual experiments (12 pages). Ordering information is given on any current masthead page.

(71) James, B. R.; Rempel, G. L. *Can. J. Chem.* **1966**, *44*, 233.